

CHARGED-PARTICLE SPECTROSCOPY: A NEW DIAGNOSTIC FOR INERTIAL FUSION IMPLOSIONS

T. W. Phillips R. D. Petrasso*

M. D. Cable T. C. Sangster

D. G. Hicks* F. H. Se'guin*

C. K. Li* J. M. Squires**

Introduction

The prospect of ignition in inertially confined fusion (ICF) targets challenges our ability to diagnose fuel conditions within the implosion. A collaboration of efforts at Lawrence Livermore National Laboratory (LLNL), Massachusetts Institute of Technology (MIT), and the University of Rochester (UR) is developing the technique of charged-particle spectroscopy to help meet the challenge. This diagnostic technique will

measure signals sensitive to the yield, areal density (fuel and core), and asymmetry of implosions.¹ Such measurements will help guide the achievement of fusion pellet ignition. Table 1 illustrates the variety of fusion reaction products that can be measured by the technique of charged-particle spectroscopy to provide a detailed picture of conditions in the fusion implosion.

Depending on the yield and density attained in compression, various charged-particle reaction products will

TABLE 1. Nuclear reactions and reaction products from fusion reactions.

Reaction type	Reactions	Observed ^a in spectrometer data
Primary fusion reactions	$D + D \rightarrow T$ (1.01 MeV) + p (3.02 MeV) $\rightarrow n$ (2.45 MeV) + ^3He (0.8 MeV) $D + T \rightarrow \alpha$ (3.5 MeV) + n (14.1 MeV) $D + ^3\text{He} \rightarrow \alpha$ (3.6 MeV) + p (14.7 MeV)	T, p α α, p
Secondary fusion reactions	^3He (0.82 MeV) + D $\rightarrow \alpha$ (6.6–1.7 MeV) + p (12.5–17.4 MeV) T (1.01 MeV) + D $\rightarrow \alpha$ (6.7–1.4 MeV) + n (11.9–17.2 MeV)	
14.1-MeV neutron knock-ons	n (14.1 MeV) + p $\rightarrow n' + p$ (\leq 14.1 MeV) n (14.1 MeV) + D $\rightarrow n' + D$ (\leq 12.5 MeV) n (14.1 MeV) + T $\rightarrow n' + T$ (\leq 10.6 MeV)	D T
30.8-MeV tertiary reaction chain	D + T $\rightarrow \alpha$ (3.5 MeV) + n (14.1 MeV) n (14.1 MeV) + D $\rightarrow n' + D$ (\leq 12.5 MeV) D (12.5 MeV) + ^3He $\rightarrow \alpha + p$ (\leq 30.8 MeV)	(step 1) (step 2) (step 3)

^aIn this column, p = protons, D = deuterons, T = tritons, and α = alphas

*Massachusetts Institute of Technology, Cambridge, MA

**University of Rochester, Rochester, NY

escape the compressed fuel and can be exploited for diagnostic measurements. The reaction products include primary products, such as protons in deuterium-deuterium (DD) fusion at low areal density. As areal density increases, higher-energy neutron knock-on products or secondary reaction products can be detected. At still higher areal density, energetic tertiary protons with birth energies from 27 to 30.8 MeV will characterize the compressed fuel of igniting implosions. Areal density measurements in different directions can be made with multiple spectrometers to determine the symmetry of the final fuel configuration. Measurement of Doppler broadening of the spectra of these charged particles will provide information on the temperature of fusion reactants.

Diagnostic Technique

The challenge of determining the energy spectra of protons, deuterons, tritons, or alphas from an ICF target is that for every particle, there are two quantities to be measured: energy and mass. To determine these independent unknowns, two measurements must be made. The spectrometer resolves this degeneracy, with a 7.6-kG dipole magnet to disperse the particles in momentum before they are detected, enabling the position of the particle event in the detector plane to be used as one measurement and the strength of the detection signal as the second. For example 3-MeV protons, 1-MeV tritons, and 3-MeV alphas follow the same path through the magnetic field, but they deposit quite different energies in a charged-coupled-device (CCD) detector or make different-sized tracks

in CR-39 plastic film.² Thus, the two independent measurements necessary to determine mass and energy are provided. Figure 1 shows the layout of the proposed magnet and detector system.

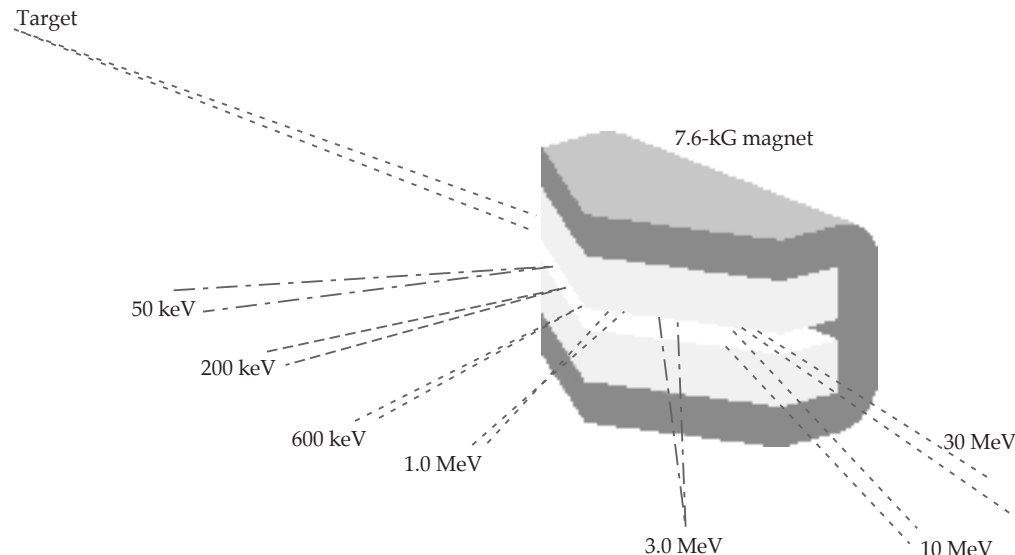
Spectrometer Design

The design of the magnet was driven by the need to view a particle spectrum from 1-MeV protons up to 10.6 MeV, to maximize the particle signal, and to be compatible with the UR Omega experimental facility. From such considerations, the 7.6-kG Nd-Fe-B dipole magnet shown in Figure 2 was constructed by Dexter Corporation.³ The pentagonal shape was necessary to allow the magnet to be positioned close to the target without obstructing the laser beams. The magnet has a 2-cm gap with better than 2% field uniformity in its central region. Use of 1.5-cm-thick shunts to smooth edge fields reduces fringing fields to 50 G at 7 cm from the magnet.

Instrumentation

Various detectors are being considered for the focal plane of the spectrometer. CR-39 track detectors are being used in the development of this diagnostic to establish its utility with minimum development effort and to obtain useful data in a radiation and electrically noisy environment. In parallel, a CCD array is being tested as an alternative focal plane detector. Preliminary data will be obtained by placing track detectors and one or two CCDs in the detector

FIGURE 1. Concept for charged-particle spectrometers (CPSs), showing how particles from a target implosion follow different trajectories through a magnet. The magnet separates particles according to momentum/charge. Particle detection and energy measurement (to uniquely identify the species and energy) are accomplished in spectrometer CPS-1 by CR-39 track detectors. CR-39 will also be used initially in a second spectrometer (CPS-2), but the detector will eventually be augmented by CCDs.
(08-00-1198-2441pb01)



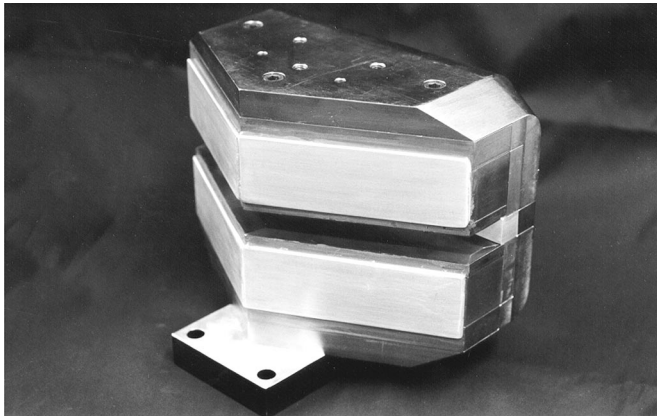


FIGURE 2. One of two identical 7.6-kG magnets fabricated for charged-particle spectrometers CPS-1 and CPS-2. The longest dimension of the magnet is 28 cm, and the gap width is 2 cm. This magnet weighs ~73 kg, and the force between the poles is 2900 kg. Although deployed in the Omega experiment, preliminary studies indicate that it is also suitable for a National Ignition Facility (NIF) charged-particle spectrometer. (08-00-1198-2439pb01)

plane of the magnet. Because the energy resolution of CR-39 film is poor (compared to that of CCDs), the track-based spectrometer will derive its energy resolution from the magnet. The presence of the magnet removes many of the limitations placed on CR-39 detectors in previous studies of knock-on, charged-particle spectra.

CCDs are extremely sensitive detectors of radiation and can easily detect individual charged particles in the MeV range, which deposit 10 to 100 times as much energy as x rays of a few keV. Unlike x rays, charged particles deposit their energy along their entire path through silicon, allowing them to be detected with 100% quantum efficiency. However, because the sensitive depth of a typical back-illuminated CCD is usually no more than 10 to 15 μm , and because light ions in the MeV range have a range of tens to hundreds of microns in silicon, only a fraction of the incident particle energy is recorded by the device. Nevertheless, through the use of well known stopping formulas, such as the Bethe–Bloch formula, and a known value for the sensitive depth, the energy recorded by the CCD is a direct measure of the incident particle energy for a given particle type.

The positioning of a particular CCD in the dispersed particle beam exiting the magnet determines the energy window that it will see, as shown in Figure 1. Within this restricted energy window, it is possible to uniquely attribute every particle event to a proton, deuteron, triton, or alpha at a specific

energy, breaking the degeneracies that existed without the magnet (where the detector would see all particles at all energies).

The Integrated System

Figure 3 is a diagram of the integrated magnet and CCD system. The support module mounted to the vacuum chamber wall allows the magnet entrance slit to be placed as close as 60 cm from the target. Much of the structure volume and region outside the structure, between the magnet and target, is filled with lead-impregnated, borated polyethylene (Pb–B–PE) to thermalize and capture a substantial fraction of the copious direct and scattered neutrons and gammas generated by the target. A beam dump is incorporated to minimize the number of scattered neutrons and gammas from the direct line of sight. For high-yield shots, the entire magnet and CCD system can be retracted, whereas for low-yield shots, the magnet entrance slit is adjustable up to 2 cm wide and 1 cm high. The slit is covered by a light-tight, 25- μm Be window to prevent laser and other light sources in the visible and near-visible range from flooding the detectors. In addition, this window (and other insertable windows) will allow the entire diagnostic system to maintain a vacuum separate from that of the target chamber, enabling easy access into the diagnostic area when maintenance is required. Seven 512 \times 512 CCDs are placed in the exit plane, as shown, to cover the

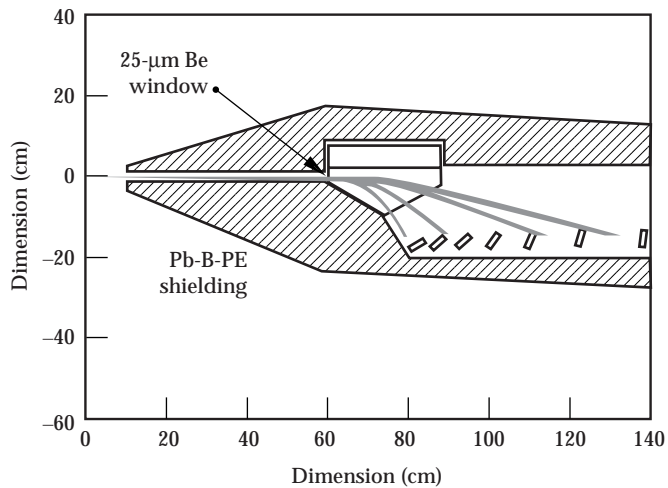


FIGURE 3. The CCD system, with approximate dimensions shown in centimeters. To minimize direct and scattered neutron and gamma noise, large amounts of Pb–B–PE shielding will be incorporated. (08-00-1198-2442pb01)

energy range from 1-MeV protons up to 10.6-MeV tritons. Each CCD is cooled to about -20°C using thermoelectric coolers. The CCDs and their electronics are custom configured to allow the arrays to be placed as close together as possible, minimizing dead space. Data is transferred via fiber-optic cables to minimize electronic pickup.

Predicted Performance

Energy Resolution

The energy resolution of this device may be determined by either the detectors or the magnet. A conservative estimate puts the total CCD resolution at better than 5%. For a slit width of 5 mm, the magnet resolution varies from 1% at low energies to 9% at high energies. For this and smaller slit widths, the magnet provides resolution comparable to that of the CCD. With CR-39 track detectors at the focal plane, the mass is well determined, but there is little energy information, so the magnet resolution dominates.

Operating Yield

For lower-yield experiments, the diagnostic will operate at 60 cm from the target with a 1-cm-high by 2-cm-wide entrance slit, giving a solid angle of 4.4×10^{-5} steradians. At a yield of 10^9 deuterium-tritium (DT) neutrons and a μR of 10 mg/cm^2 , ~100 knock-ons will be detected. When the neutron yield is 10^{13} , a 1-cm-high by 1-mm-wide magnet entrance slit placed at the vacuum wall (160 cm from the target) will result in detection of 10^4 knock-ons when $\mu R = 10 \text{ mg/cm}^2$. This diagnostic can thus span four orders of magnitude in DT yield.

Signal-to-Noise Ratio

The main sources of noise in the system will be from the 14-MeV neutrons and their associated gammas—both direct and scattered. Because of the complex nature of the interactions of neutrons with the surrounding target chamber, it is extremely difficult to precisely predict the noise sensitivity of the CCD to this type of radiation environment. To obtain an estimate of the noise levels, however, the CCDs were exposed to 14-MeV neutrons from the MIT Cockcroft-Walton accelerator, and an “effective” neutron sensitivity of 2×10^{-3} was obtained. A simple calculation of the number of direct neutron interactions with the sensitive region of the CCD predicted a sensitivity lower by a factor of 20, and we believe that the discrepancy is

caused by neutron-induced gamma interactions. However, because most of these interactions produce a small response in the CCD, the events will fall below the charged-particle signal levels of interest, and they may be rejected.

Furthermore, the magnet provides an additional means of noise rejection. Because each CCD is restricted to viewing a narrow particle-energy window by virtue of its position in the dispersed particle beam, any noise events that occur outside the designated energy window can be discarded. Thus, a calculation of the instrument signal-to-noise ratio using the neutron data must take into account the spectral quality of neutron interactions, and not just the absolute sensitivity. In addition, Monte Carlo simulations and experimental measurements have indicated that 60 cm of Pb-B-PE shielding attenuates the neutron flux by more than a factor of 100.

From these considerations, the signal-to-noise ratio for a DT yield of 10^{11} and $\mu R = 10 \text{ mg/cm}^2$ with the 5-mm \times 1-cm magnet slit at 60 cm from the target can be calculated. For the 512×512 CCD in the high-energy part of the dispersed beam, 350 tritons (from 6.2 to 10.6 MeV) and 200 deuteron knock-ons (from 9.3 to 12.5 MeV) will be detected. The number of neutron and associated gamma events in these ranges, which were predicted on the basis of CCD neutron measurements, give signal-to-noise ratios of 160:1 for tritons and 400:1 for deuterons.

CCD Damage

While testing the response of 512×512 CCDs to protons, alphas, and neutrons, we have seen an increase in the dark-current level of individual pixels with irradiation levels of $\sim 10^9/\text{cm}^2$, probably due to single-hit damage. On a cooled device that is read out rapidly, the effects of such increased dark current are negligible. The levels of irradiation on the Omega chamber are expected to be much less than those to which the device has already been exposed.

For CR-39 plastic track detectors, noise and damage are minor concerns solved by care in handling and etching the material. This fact makes CR-39 a good choice for demonstrating the utility of the technique during the test phase.

Testing the Technique

During the charged-particle spectrometer’s design and construction, tests were conducted of the response of various components to charged particles produced in fusion reactions and the chamber environment of radiation and electrical noise. The first tests employed

small accelerators to produce the charge particles of interest. Both CR-39 and CCD detectors were exposed to protons in the range from 1 to 14 MeV. For CR-39, our tests helped in developing etching and imaging techniques, which gave good sensitivity and reliability for measuring track number and size distributions. The track size distributions were calibrated with particle energy, and automatic scanning, sizing, and counting algorithms were developed.⁴ Similar tests on CCDs established their utility for determining particle energy and mass. Tests on the CCD arrays provided confirmation of the calculated response to charged particles and calibrated them.⁵

Tests were then carried out on fusion implosion experiments, beginning with CR-39 exposed to DD and DT implosions at the LLNL Nova facility. Track sizes consistent with those obtained for accelerator exposures, as well as consistent with the yield observed in neutron diagnostics, gave us confidence in CR-39 as a detector. The DT exposures were dominated by neutron-induced tracks, which made clear the need for good shielding in the spectrometer design.⁴ Tests of the CCDs on fusion experiments were carried out at the UR Omega facility. These tests demonstrated that neutron-induced noise could be reduced by shielding

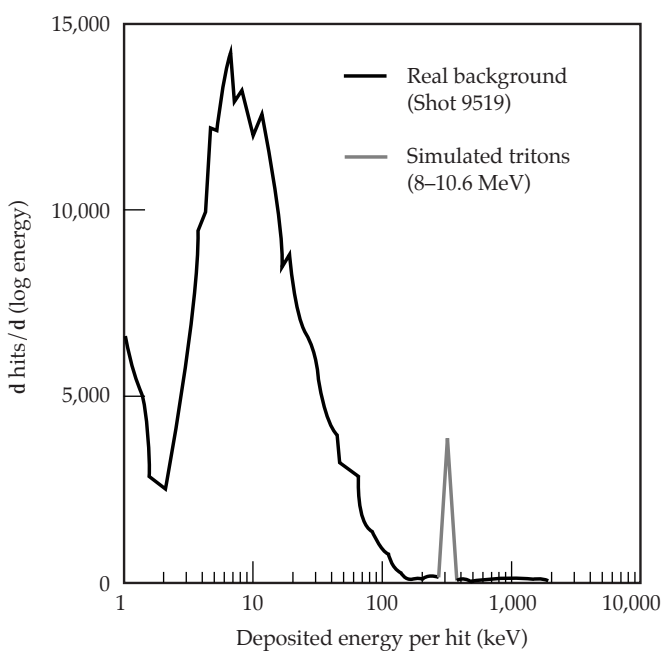


FIGURE 4. Simulated CCD spectra. To estimate what data may actually look like for various CCDs in the magnet-based spectrometer during real shots, calculated spectra for particles of interest were superposed on an actual noise spectrum taken during an Omega DT shot with neutron yield = 4.1×10^{11} . The plot represents the expected spectrum at an appropriate CCD position. (08-00-1198-2443pb01)

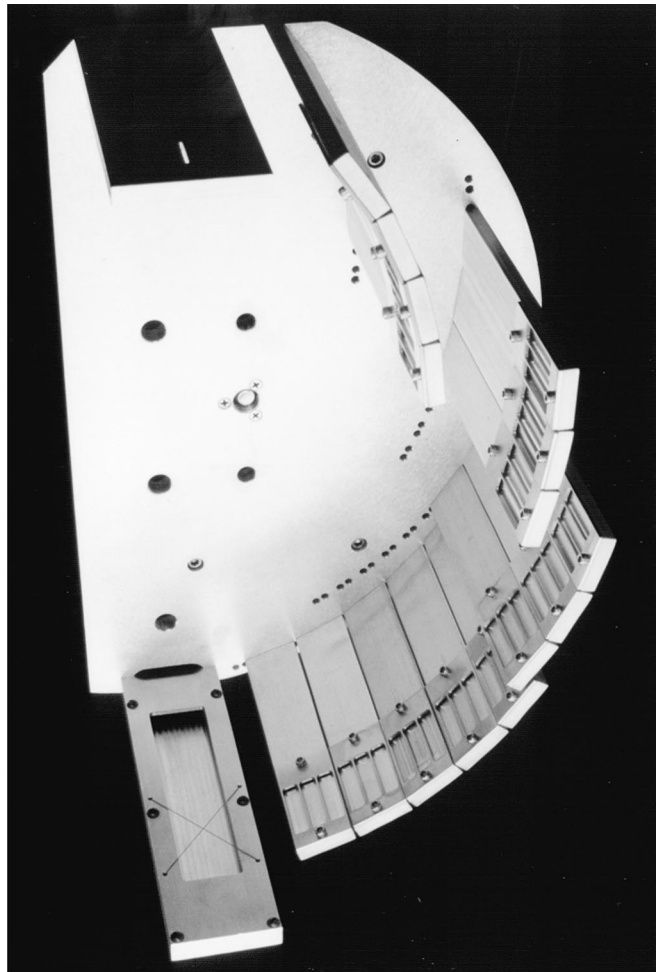


FIGURE 5. The CR-39 detector holder (seen from below) for CPS-1. Fifteen finger plates that support the CR-39 film are assembled in four rows. At the top of the picture is a small, adjustable entrance slit. On the bottom, a finger plate with crossed wires holds x-ray film used to monitor alignment. (08-00-1198-2444pb01)

that would fit within the space available between the laser beams. Detection of fusion charge particles in the presence of this background was simulated using the measured neutron-induced background and adding accelerator-produced, charged-particle data, as shown in Figure 4. The detection of charged particles from a fusion implosion must await the installation of CCDs in the focal plane of the spectrometer.

Full systems tests with two magnets have been carried out on the UR Omega facility using CR-39 as the focal plane detector. A holder shown in Figure 5, which permits easy and reproducible positioning of the CR-39 film in the focal plane of the magnet, was constructed. Exposures have been obtained with DD, D³He, and DT implosions. An example of the performance of the magnet and CR-39 in sorting out

the multiple species from a D³He exposure is shown in Figures 6 and 7. In Figure 6, the mix of alphas, tritons, and protons can be seen in the different track sizes. The histogram in Figure 7 demonstrates identification and counting by the automated system. Typical DT α , DD p, DD t, D³He p, and knock-on spectra from these tests are shown in Figure 8. Parameters such as yield, ion temperature, and areal density can be extracted from analyses of these spectra and compared with such parameters obtained by other techniques. The details of analyses and comparisons will be the subject of a future paper.

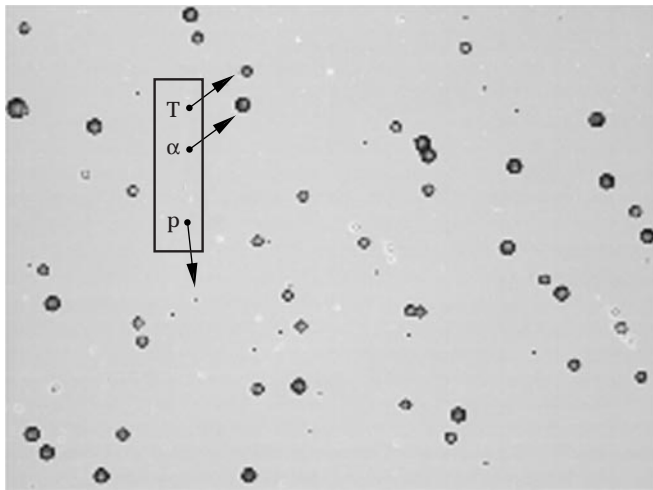


FIGURE 6. DD proton, DD triton, and D³He alpha tracks in CR-39 from Shot 11585 with a D³He target. This piece of CR-39 was positioned at finger D5 in the spectrometer, behind a 6- μm Al filter. The ~3.3-MeV DD protons and ~1.1-MeV DD tritons have the same position on the focal plane of the magnet. In addition, due to the energy spread of D³He alphas (some having energies down to 3.3 MeV), all three types of particle actually appear at this position. However, each particle type can be distinguished easily by its diameter, which is a function of stopping power. This image emphasizes a key concept of the new spectrometer: different charged fusion products with the same magnetic paths have very different stopping powers, allowing unique particle identification.

(08-00-1198-2440pb01)

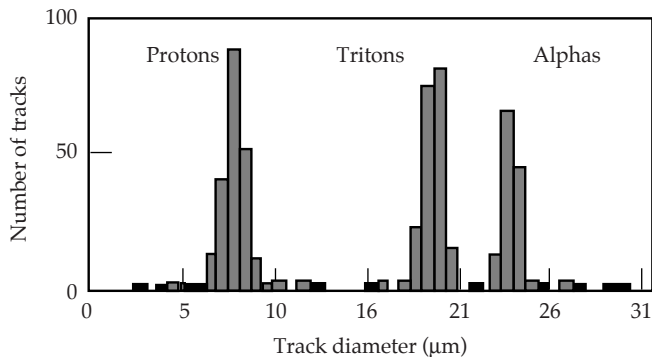


FIGURE 7. A track diameter histogram for the “triple degeneracy” position around the region shown in Figure 6. In this region, DD protons, DD tritons, and some lower-energy D³He alphas all have the same magnetic paths. However, their differing stopping powers allow each particle type to be uniquely identified. At these energies (3.3 MeV for protons, 1.1 MeV for tritons, and 3.3 MeV for alphas), the alphas have the largest stopping power, and the protons the smallest. (08-00-1198-2445pb01)

Conclusions

A novel diagnostic for laser fusion implosions has been developed through a collaboration of LLNL, MIT, and UR scientists. The technique of charged-particle spectroscopy employs a permanent magnet spectrometer and permits the use of various detection techniques to measure the spectra of charged, energetic nuclear reaction products emitted during the fusion implosion. Properties of the fusion plasma, such as yield, areal density, temperature, and symmetry, may be inferred from the charged-particle spectra. Testing of the technique on fusion implosions has successfully demonstrated its utility as a diagnostic tool for these fusion parameters. Qualitative agreement with other yield measures has been demonstrated. Detailed analyses and comparisons will be the subject of a future paper.

Notes and References

1. R. D. Petrasso, et al., *Phys. Rev. Lett.* **77**, 2718 (1996).
2. A. P. Fews, *NIM* **B71**, 465–478 (1992).
3. Dexter Corporation, Magnetic Materials Division (PERMAG), 48460 Kato Rd., Fremont, CA, 94538.
4. T. W. Phillips et al., *Rev. Sci. Inst.* **68**, 596 (1997).
5. C. K. Li et al., *Rev. Sci. Inst.* **68**, 593 (1997).

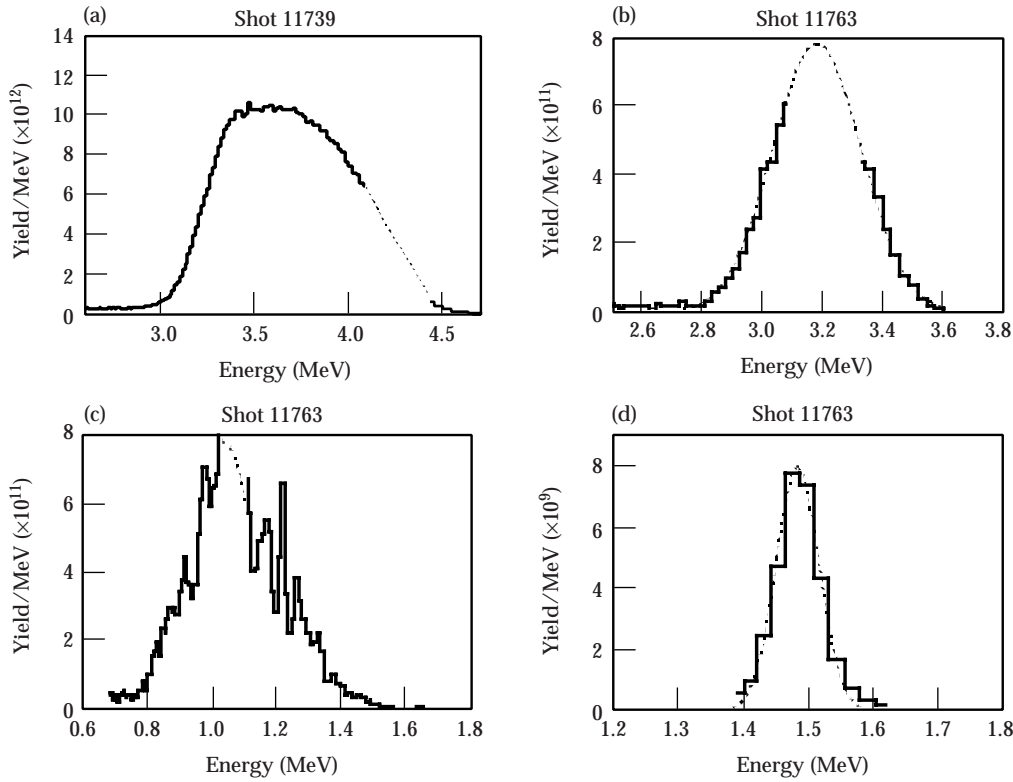


FIGURE 8. Typical spectra obtained from DT, DD, and D^3He shots on Omega with CR-39 detectors in the spectrometer focal plane. (a) DT alpha spectrum from shot 11739. From the Gaussian fit, the mean energy was 3.67 MeV ($\pm \sim 1\%$) with a width of 0.39 MeV, while the yield was 1.01×10^{13} ($\pm 15\%$). (b) DD proton spectrum from Shot 11763. From the Gaussian fit, the mean energy was 3.18 MeV ($\pm \sim 1\%$) with a standard deviation of 0.15 MeV, while the yield was 2.89×10^{11} ($\pm 15\%$). In this instance, the proton “line” happened to straddle the 3-mm dead space between finger positions D3 and D5, as indicated by the gap in the spectrum. (c) DD triton spectrum from Shot 11763. From the Gaussian fit, the mean energy was 1.08 MeV ($\pm \sim 1\%$) with a standard deviation of 0.15 MeV, while the yield was 2.55×10^{11} ($\pm 15\%$) (consistent with the proton yield). (d) D^3He proton spectrum from Shot 11763. From the Gaussian fit, the mean energy was 14.85 MeV ($\pm \sim 1\%$) with a standard deviation of 0.33 MeV. The yield was 6.57×10^9 . The width of the peak is slit-resolution-limited, because the physical width of this proton line (2 mm) is comparable to the slit width (1 mm). The protons were ranged through 1000 μm and 1100 μm of aluminum to make them easily detectable in CR-39. (08-00-1198-2446pb01)